# Research Proposal on Automobile Direct Time of Flight LiDAR SoCs

Zhen Xu

August 18, 2024


## Abstract

Autonomous driving is one of the most cutting-edge research topics in today's and future scientific communities. Measurement of velocity and its direction are key technologies to ensure the safety of autonomous driving. Among all environmental perception technologies in autonomous driving, LiDAR has advantages such as good distance range, high image resolution and excellent environmental robustness, indicating its great potential for future development. Compared with other types of LiDARs, dToF LiDARs offer superior performance in high resolution and long-range capability. Over the past twenty years, with the application of SPADs and TDCs in dToF LiDARs, and the maturation of new technologies such as 2D-SPAD Arrays and 3D Integration, dToF LiDARs have continually improved in performance and have seen extensive commercialization. This research aims to propose and design a new generation of dToF LiDARs to achieve better performance than previous models.


## I Research Background

Humans have superior sensory organs and decision-making mechanisms compared to most modern hardware and software systems. However, people occasionally make extremely naive mistakes that can lead to irreversible consequences, particularly while driving. Since human errors cannot be entirely eliminated, advanced driver-assistance systems (ADAS) technology has been developed to address these errors.

Today, many companies are actively employing autonomous driving technology. For example, Mercedes-Benz has received permission to conduct Level 4 autonomous driving tests on designated city roads[1], and Honda plans to launch a driverless taxi service in Tokyo by 2026, which will be among the world's first commercial driverless taxi services[2].

To achieve autonomous driving, high-quality depth sensors are essential. Ref.[3] summarized the typical depth sensors used in ADAS systems, as shown in Table 1. Although LiDAR is expensive due to its mechanical scanning components, it is the only depth sensor that provides both high resolution and long-distance measurements.

Compared to other LiDAR technologies, dToF LiDAR offers significant advantages in autonomous driving, particularly in terms of high precision and long-range capability. dToF LiDAR directly measures the flight time of laser pulses, providing extremely high measurement accuracy and resolution, which is crucial in complex driving environments. Additionally, dToF LiDAR excels in long-distance detection, enabling accurate capture of distant obstacles and environmental information even at high speeds, thereby enhancing the safety and responsiveness of autonomous driving systems. Although dToF LiDAR has relatively high power consumption and cost, its outstanding performance makes it an indispensable sensor technology in the field of autonomous driving.

| Features | Ultrasonic | Stereo Camera | mm-wave Radar | LiDAR |
|---|---|---|---|---|
| Distance | ☹ | ☹ | ☺ | ☺ |
| High image resolution | ☹ | ☺ | ☹ | ☺ |
| Environment robustness | ☺ | ☹ | ☺ | 😐 |
| Cost | ☺ | ☺ | ☺ | ☹→😐 |

**Table 1:** A distance sensor used in typical ADAS systems is shown. There is a trade-off between cost and performance.

# II Literature Review

## A. First Generation LiDARs

Velodyne's rotational LiDAR achieves high-quality depth sensing through the vertical stacking of laser and receiver boards. Although it was released during the early development of ADAS LiDAR, it has demonstrated excellent performance, such as the VELODYNE HDL-64E, which has a detection range of 120 meters with a distance error of less than one inch[4].

As shown in Figure 1 from Ref.[3], the first-generation LiDAR uses an APD as the photodetector. The APD output is amplified by TIA and VGA, then quantized by a high-speed ADC, and the Time of Flight (ToF) is calculated in the digital processor. Although the first-generation LiDAR achieved relatively good performance, this implementation required many discrete components, resulting in high cost and fragility. Additionally, improving resolution without increasing cost is difficult because the number of components directly impacts the resolution. Furthermore, APDs are still inadequate for meeting the 200-meter detection range required for autonomous driving technology.

## B. SPADs

Ref.[5] explores the properties of Single Photon Avalanche Diodes (SPADs) and the basic architecture of digital pixels built with them. SPADs are highly sensitive photodetectors capable of single-photon detection and are widely used in next-generation direct Time-of-Flight (dToF) LiDAR systems due to their sensitive characteristics.

SPADs are usually biased far above $V_{bd}$ and operate in the so-called Geiger mode. Unlike in linear mode photodiodes, in SPADs, the signal amplitude does not provide intensity information since a current pulse has the same amplitude whether it was triggered by a single photon or multiple photons. Intensity information is obtained by counting the pulses during a certain period of time or by measuring the mean time interval between successive pulses.

The digital pixel proposed in Ref.[5] is shown in Figure 2. It can convert very weak photon

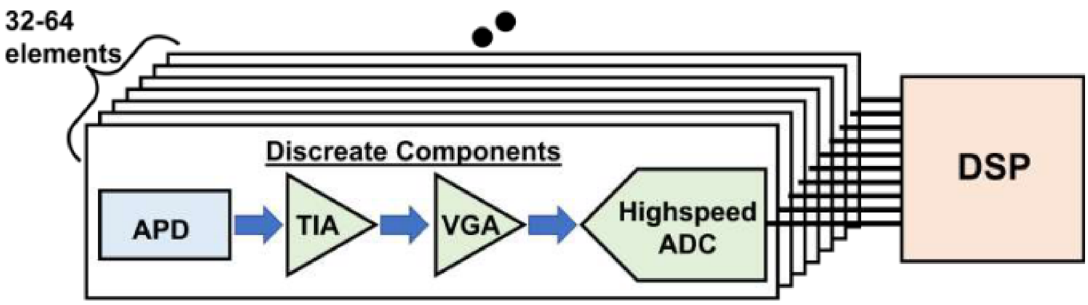


**Figure 1:** System diagram of first-generation LiDAR.

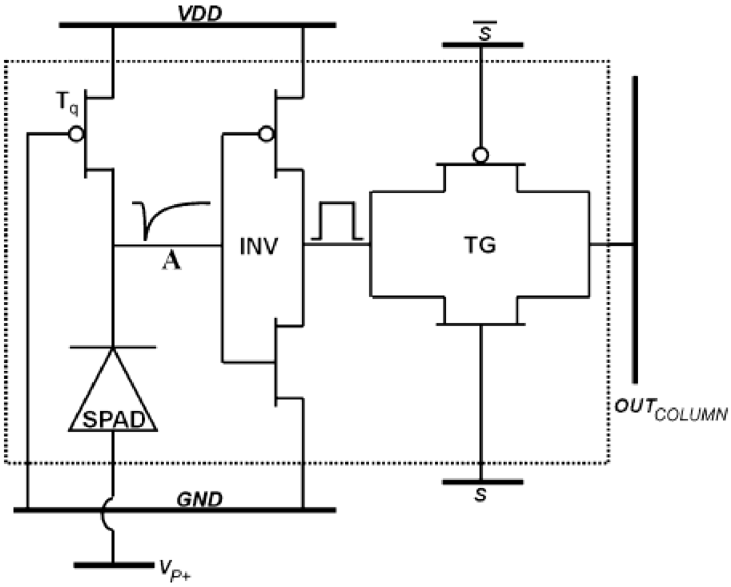


**Figure 2:** Schematic of 5 T digital pixel.

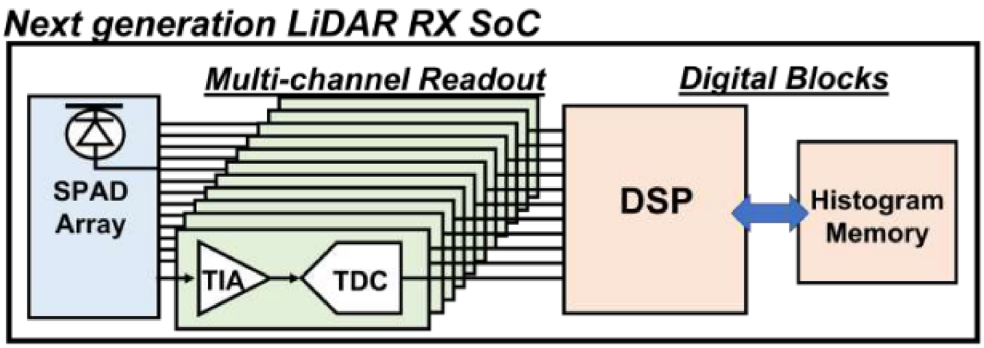


**Figure 3:** System diagram of next-generation LiDARs.

incidence into voltage pulses and is widely used in current dToF LiDAR systems.

## C. Next Generation LiDARs

Compared to the first-generation LiDARs, Ref.[6] and Ref.[7] have made significant structural improvements in four main aspects. First, Ref.[6] and Ref.[7] use SPADs instead of APDs as in Ref.[4]. SPADs greatly enhance the long-range performance of the LiDARs because Their strong amplification enables the detection of single photons and faint returning lasers during long-distance measurements. Second, TDC-based readout circuitry is used because implementing several tens or hundreds of high-speed ADCs on an SoC is difficult due to the small area. Third, special signal processing circuits are employed to distinguish between background light (BG) and signal photons. Isolated photon events are more likely to originate from uncorrelated background light, which has disparate arrival times, while signal photons are confined to the duration of the laser pulse and thus exhibit a significantly higher probability of correlation. Consequently, the coincidence detection circuits in signal processing systems generate ToF evaluation trigger signals only when two or more photons are detected simultaneously within a given short time frame. In Ref.[7], the coincidence detection circuits are implemented using analog methods, while in Ref.[6], they are implemented using digital circuits. Finally, in Ref.[6] and Ref.[7], the LiDAR signal-to-noise ratio (SNR) was improved by histogramming the TDC output of multiple measurement results. Specifically, the TDC is triggered only when the accumulation of SPAD firing signals exceeds a certain threshold. This approach addresses the following issues: 1) Recording all incoming sunlight events would make the histogram memory very large; 2) Due to the finite TDC reset time, the TDC might miss the laser if triggered by sunlight. By adding a threshold to the TDC trigger, both problems can

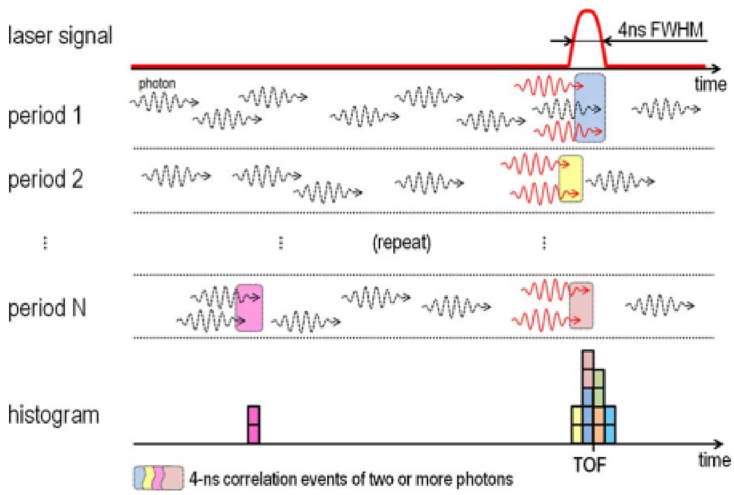


**Figure 4:** Diagram of the spatiotemporal-correlated photon counting technique utilized to reject uncorrelated events such as photons from the ambient light. The start times of the depicted waveforms coincide with the laser pulse emission time within each repetition period. The hypothetical detection time of photons within a pixel is illustrated by wave-packet-shaped symbols. The black symbols represent photons from the uncorrelated background light, whereas the red symbols represent photons from the laser signal. Note that despite an incident optical signal-to-background ratio much lower than unity, the resulting histogram suggests that the ToF can be determined reliably

be simultaneously resolved.

The system diagrams for Ref.[6] and Ref.[7] are shown in Figure 3 from Ref.[3]. The schematic for distinguishing signal photons from ambient light in Ref.[7] is shown in Figure 4.

## D. TDC/ADC Hybrid Architecture

In Ref.[7], since the TDC is triggered only when the SPAD firing signal exceeds a certain threshold, this accumulation method is not effective when the returning laser is very weak at long distances. If we could directly accumulate the raw SPAD waveforms, the LiDAR could effectively utilize information below the accumulation threshold, but this setup would require an ADC as the readout circuit.

Ref.[8] solved this problem by adopting a hybrid readout circuitry, which switches between ADC and TDC for long and short distances, respectively. In short-distance measurements, where high distance resolution is needed and the signal-to-noise ratio (SNR) of the returning laser is sufficient, the TDC is used. Conversely, for long-distance measurements (greater than 20 meters) where the SNR is lower, the ADC directly reads the SiPM waveform, and accumulation is performed at the raw waveform level. Additionally, Ref.[8] used Smart Accumulation Technique to address the issue of image quality degradation in the simple accumulation, where a group of pixels observing different targets can lead to decreased image quality. The pixel data (raw ADC output) is preprocessed to mark peak level (PL) and floor level (FL), as shown in Figure 5 from Ref.[8]. The amplitude range of the ADC depends on the number of captured photons, so PL is strongly correlated with the target's reflectance and distance. Furthermore, since sunlight not only directly enters the LiDAR but also enters through reflections from the target, FL is also strongly correlated with the target. Therefore, the Smart Accumulation Technique (SAT) accumulates corresponding pixels only when the correlation between PL, FL, and the target (MP) exceeds an appropriate threshold, significantly reducing the occurrence of accumulated data showing two peaks due to a group of pixels observing different targets.

Ref.[9] builds upon Ref.[8] by implementing a Dual-Data-Converter (DDC) based on a voltage-controlled oscillator (VCO). By integrating ADC and TDC functionalities into a single circuit, Ref.[9] reduces the number of circuit modules needed for implementing the LiDAR Analog Front End (AFE). Through the design of a 40-channel LiDAR SoC based on the DDC, Ref.[9] achieves a distance range of 225 meters, with distinguished image quality, high resolution, and a compact AFE area.

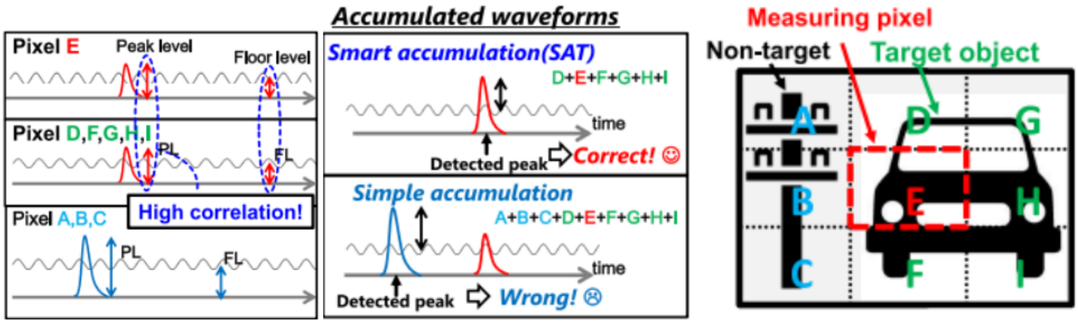


**Figure 5:** Raw output of each pixels or the ADC output waveforms. When the pixels "watch" the same object, its PL and FL show high correlation and SAT will use such information to classify the objects. With SAT, only the pixels "watching" the same object are accumulated.

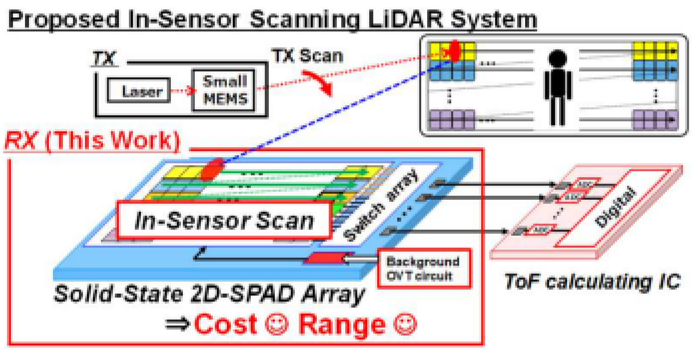


**Figure 6:** Proposed LiDAR system with In-Sensor Scanning Self-calibrated 2D-SPAD array.

## E. 2D-SPAD Array Approach

Traditional scanning 2D LiDAR uses mechanical mirrors for 2D scanning to obtain 2D distance images. Since the receiver (RX) utilizes one-dimensional single-photon avalanche diodes (SPADs), not only the transmitter (TX) but also the receiver needs to use mirror scanning to direct the reflected light to the receiver. To achieve a distance range of 200 meters, a large mirror aperture is usually required, making mechanical multi-facet mirrors bulky and costly.

To eliminate the cumbersome multi-facet mirrors in the receiver's scanning system, Ref.[10] proposes a 2D SPAD array with an in-sensor scanning mechanism. Figure 6 illustrates the in-sensor scanning (ISS) 2D SPAD array proposed in Ref.[10]. By performing scanning of the receiver within the 2D SPAD array, the expensive mechanical mirrors in the receiver system are removed.

To maximize pixel resolution within a feasible chip size, Ref.[10] employs an active quenching (AQ) reset circuit as described in Ref.[11]. The AQ circuit detects the SPAD trigger via a comparator and then quickly charges the SPAD through an active switch after a short delay; the SPAD can be triggered again after charging. Compared to passive quenching (PQ) SPADs, AQ SPADs have a shorter dead time. Ref.[10] achieves 8x higher pixel-resolution including the AQ circuitry overhead.

## F. 3D Integration Approach

As the number of pixels increases, the interchip connectivity becomes complex. Also, considering the area required for the readout circuit, which is traditionally located on the same plane as the sensor, explains why SPAD arrays have been limited in terms of fill factor (F.F) and pixel unit size up to the present.

To address this issue, Ref.[12] proposes a LiDAR SoC using a 3D integration approach and back-illuminated (BI) structure, as shown in Figure 7. The benefits of this structure are as follows: first, 3D integration allows SPAD and DSP chips to be fabricated in their respective suitable processes. Second, the high-density 3D interchip connections support wiring for a larger number of SPADs. Since simple SPADs can replace SiPMs, area-efficient TDCs can be used as the readout circuit. Finally, by applying microlenses and back-illuminated technology to SPADs, Ref.[12] demonstrate

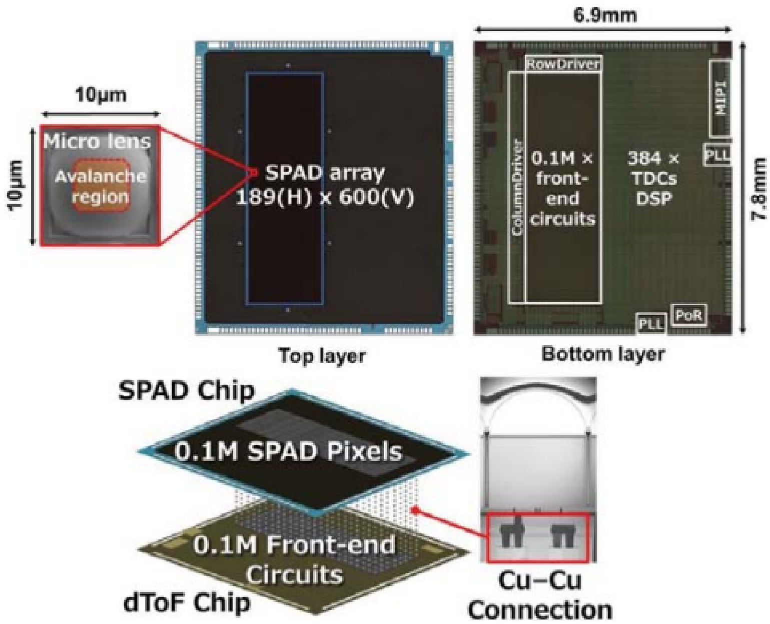


**Figure 7:** Die micrograph (top) and cross-sectional view of stacked SPAD with Cu-Cu connections (bottom).

| | Ouster OS2[13] | InnovizTwo[14] | Luminar Hydra[15] | Valeo's SCALA 2[16] |
|---|---|---|---|---|
| Distance range | 200 m/350 m | 120 m/170 m | 250 m | 100 m/200 m |
| Field of View | Vertical: 22.5º (+11.25° to -11.25°) Horizontal: 360° | 120ºx28.8º | 120ºx30º | 133ºx10º |
| Vertical Resolution | 32/64/128 channels | 0.05º | 0.03º | 0.6º |
| Horizontal Resolution | 512/1024/2048 channels | 0.1º | 0.07º | 0.125º for +/-15º 0.25º for +/-15º to+/-66.5º |
| Range Resolution | 0.1 cm | 1 cm | 1 cm | <1 cm |
| Target Reflectivity | 10%/80% | 10%/50% | <10% | 10%/80% |
| Laser Wavelength | 865 nm | 905 nm | N.A. | 905 nm |
| 1 sigma error @ max distance | <10 cm | 15 cm | N.A. | N.A. |
| SoC power consumption state | 18 - 24 W | 19 W | 55 W | <10 W in steady |
| Background light | 100 klx | N.A. | N.A. | N.A. |
| FPS | 20 FPS | 20 FPS | 1-30 FPS | 25 FPS |

**Table 2:** Performance comparison of some LiDARs on the market.

that the photon detection efficiency (PDE) can be significantly improved to 22% at a wavelength of 905 nm, which is almost a 2x increase from conventional SPADs.

## G. LiDARs on the market

After conducting the research, I have listed the performance specifications of some LiDARs on the market in Table 2. The application and improvement of LiDARs in the industry are significant for determining future research directions.

# III Research Aim

The purpose of this research is to, **first**, conduct a literature review to indicate the technical requirements of environment perception technologies in autonomous driving systems. **Second**, calculate the necessary parameters of the LiDAR system for autonomous driving. **Third**, propose and design a dToF LiDAR architecture that is suitable for autonomous driving with excellent detection range, resolution, low power consumption, and low cost. **Finally**, the LiDAR system will be developed, and simulations and experiments will be conducted to verify whether it meets the required specifications.

# IV Research Method

The methods I plan to use in my research are as follows:

## A. Literature Research

I plan to analyze different environmental perception technologies used in autonomous driving, with a particular focus on LiDAR systems. I will also compare different vehicle-mounted LiDAR products available today and use these insights as a reference for designing a new dToF LiDAR system.

## B. Theoretical Analysis and Design

Prior to the design phase, I will analyze and calculate the critical parameters of dToF LiDARs used in autonomous vehicles, such as distance range, accuracy, field of view, resolution, and frame rate (FPS). Following this analysis, I will use Cadence tools to design the circuit and conduct simulations to ensure the circuit achieves sufficient gain, bandwidth, swing, and other essential performance characteristics.

## C. Experiments and Simulations

After the design and fabrication, I plan to conduct experiments on distance and velocity measurements using the dToF LiDAR and perform relevant simulations to validate the system's performance for autonomous driving applications. Specifically, I intend to measure the distance range, 1 sigma error at maximum distance, and range resolution under 100 klx background light, with tests divided into two groups based on target reflectivity of 10% and 80%. The results will then be compared with the expected design goals.

# V Expected Results

There are still many technologies to be discovered in the field of vehicle-mounted LiDARs, and it has promising application prospects in autonomous driving. I hope to use the research results of the dToF LiDAR to explore ways to achieve a small, low-cost vehicle LiDAR system with outstanding performance in distance range, field of view, resolution, and other aspects.

# References


[1] *Mercedes-Benz Approved for Level 4 Driving Tests.* Aug. 9, 2024. URL: https://selfdrivenews.com/mercedes-benz-approved-for-level-4-driving-tests/.

[2] *Japan Gears Up for Autonomous Mobility as Companies Put Their Tech to the Test.* Dec. 7, 2023. URL: https://japan-forward.com/gearing-up-for-autonomous-mobility-as-companies-put-their-tech-to-the-test/.

[3] Kentaro YOSHIOKA. "A Tutorial and Review of Automobile Direct ToF LiDAR SoCs: Evolution of Next-Generation LiDARs". In: *IEICE Transactions on Electronics* E105.C.10 (2022), pp. 534–543. DOI: 10.1587/transele.2021CTI0002.

[4] "VELODYNE'S HDL-64E: A HIGH DEFINITION LIDAR SENSOR FOR 3-D APPLICATIONS". In: 2009. URL: https://api.semanticscholar.org/CorpusID:26835230.

[5] C. Niclass et al. "Design and characterization of a CMOS 3-D image sensor based on single photon avalanche diodes". In: *IEEE Journal of Solid-State Circuits* 40.9 (2005), pp. 1847–1854. DOI: 10.1109/JSSC.2005.848173.

[6] Cristiano Niclass et al. "A 100-m Range 10-Frame/s 340 $\times$96-Pixel Time-of-Flight Depth Sensor in 0.18-$\mu$m CMOS". In: *IEEE Journal of Solid-State Circuits* 48.2 (2013), pp. 559–572. DOI: 10.1109/JSSC.2012.2227607.

[7] Cristiano Niclass et al. “A 0.18-$\mu$ m CMOS SoC for a 100-m-Range 10-Frame/s 200 $\times$96-Pixel Time-of-Flight Depth Sensor”. In: *IEEE Journal of Solid-State Circuits* 49.1 (2014), pp. 315–330. DOI: 10.1109/JSSC.2013.2284352.

[8] Kentaro Yoshioka et al. “A 20-ch TDC/ADC Hybrid Architecture LiDAR SoC for 240 $\times$ 96 Pixel 200-m Range Imaging With Smart Accumulation Technique and Residue Quantizing SAR ADC”. In: *IEEE Journal of Solid-State Circuits* 53.11 (2018), pp. 3026–3038. DOI: 10.1109/JSSC.2018.2868315.

[9] Satoshi Kondo et al. “An Automotive LiDAR SoC for 240 $\times$ 192-Pixel 225-m-Range Imaging With a 40-Channel 0.0036-mm2 Voltage/Time Dual-Data-Converter-Based AFE”. In: *IEEE Journal of Solid-State Circuits* 55.11 (2020), pp. 2866–2877. DOI: 10.1109/JSSC.2020.3020812.

[10] Tuan Thanh Ta et al. “A 2D-SPAD Array and Read-Out AFE for Next-Generation Solid-State LiDAR”. In: *2020 IEEE Symposium on VLSI Circuits*. 2020, pp. 1–2. DOI: 10.1109/VLSICircuits18222.2020.9162831.

[11] F. Zappa et al. “Monolithic active-quenching and active-reset circuit for single-photon avalanche detectors”. In: *IEEE Journal of Solid-State Circuits* 38.7 (2003), pp. 1298–1301. DOI: 10.1109/JSSC.2003.813291.

[12] Oichi Kumagai et al. “7.3 A 189$\times$600 Back-Illuminated Stacked SPAD Direct Time-of-Flight Depth Sensor for Automotive LiDAR Systems”. In: *2021 IEEE International Solid-State Circuits Conference (ISSCC)*. Vol. 64. 2021, pp. 110–112. DOI: 10.1109/ISSCC42613.2021.9365961.

[13] *OS2: Long-range digital lidar sensor*. URL: https://ouster.com/products/hardware/os2-lidar-sensor.

[14] *InnovizTwo: Next-Generation, Low-Cost, Automotive-Grade LiDAR*. URL: https://innoviz.tech/innoviztwo#top.

[15] *Luminar-Hydra-Datasheet*. URL: https://levelfivesupplies.com/wp-content/uploads/2020/08/Luminar-Hydra-Datasheet.pdf.

[16] *Valeo SCALA 3D Laser Scanner (Gen 2)*. URL: https://autonomoustuff.com/products/valeo-scala-gen-2.